Expression, Localization and Functional Coupling of the Somatostatin Receptor Subtype 2 in a Mouse Model of Oxygen-Induced Retinopathy

Journal:	*Investigative Ophthalmology & Visual Science*
Manuscript ID:	IOVS-09-4472.R1
Manuscript Type:	Article
Date Submitted by the Author:	17-Nov-2009
Complete List of Authors:	Dal Monte, Massimo; University of Pisa, Department of Biology Ristori, Chiara; University of Pisa, Department of Biology Videau, Catherine; INSERM Loudes, Catherine; INSERM Martini, Davide; University of Pisa, Department of Biology Casini, Giovanni; University of Tuscia, Department of Environmental Sciences Epelbaum, Jacques; INSERM Bagnoli, Paola; University of Pisa, Biology
Keywords:	angiogenesis, hypoxia, somatostatinergic system, retinal vasculature
Abstract:	PURPOSE. In the mouse model of oxygen-induced retinopathy (OIR) somatostatin (SRIF) acting at the SRIF receptor subtype 2 (sst2) inhibits angiogenic responses to hypoxia through a downregulation of vascular endothelial growth factor. Information on the sites where SRIF-sst2 interactions take place is lacking, and downstream effectors mediating SRIF-sst2 antiangiogenic actions are unknown. METHODS. In the OIR model, retinal expression of SRIF was evaluated with RT-PCR and RIA. The bindings of [125I]LTT-SRIF-28 and [125I]Tyr3-octreotide were measured in coronal sections of the eye. With Western blot we evaluated the levels of sst2A as well as the expression and the activity of the Signal Transducer and Activator of Transcription (STAT)3. The analysis of STAT3 was performed in hypoxic mice treated with the sst2 agonist octreotide or with the sst2 antagonist D-Tyr8 cyanamid 154806 (CYN). Retinal localization of sst2A was assessed by single and double immunohistochemistry with an endothelial cell marker. RESULTS. In the hypoxic retina, both SRIF and sst2 levels as well as [125I]Tyr3-octreotide binding were downregulated. In addition, sst2A immunostaining was decreased in the neuroretina, but was increased in capillaries. Hypoxia increased both expression and activity of STAT3. This increase was inhibited by octreotide, while was strengthened by CYN. CONCLUSIONS. These data suggest that i. sst2 expressed by

	capillaries may be responsible of the antiangiogenic effects of SRIF and ii. downstream effectors in this action include the transcription factor STAT3. These results support the possibility of using sst2-selective ligands in the treatment of proliferative retinopathies and indicate STAT3 as an additional target for novel therapeutic approach.

Expression, Localization and Functional Coupling of the Somatostatin Receptor Subtype 2 in a Mouse Model of Oxygen-Induced Retinopathy

Massimo Dal Monte[1], Chiara Ristori[1], Catherine Videau[2], Catherine Loudes[2], Davide Martini[1], Giovanni Casini[3], Jacques Epelbaum[2], Paola Bagnoli[1]

[1]Dipartimento di Biologia – Università di Pisa – Via San Zeno, 31 – Pisa, Italy

[2]Institut National de la Santé et de la Recherche Medicale, INSERM-Universite´ Paris Descartes UMR 894 – 2, ter rue d'Alesia – Paris, France

[3]Dipartimento di Scienze Ambientali – Universita` della Tuscia – Largo dell'Universita` – Viterbo, Italy.

MDM and CR equally contributed to the work and are listed in alphabetical order.

Corresponding author: Paola Bagnoli, Dipartimento di Biologia – Università di Pisa – Via San Zeno, 31 – 56127 Pisa, Italy – email: pbagnoli@biologia.unipi.it

Word count: 4185

Grant information: Supported by the Italian Ministry of University and Research (MUR, PRIN, grant # 2005052312) and by the Foundation of the Cassa di Risparmi of Livorno to PB

Scientific Section: BIOCHEMISTRY/MOLECULAR BIOLOGY (BI)

PURPOSE. In the mouse model of oxygen-induced retinopathy (OIR) somatostatin (SRIF) acting at the SRIF receptor subtype 2 (sst_2) inhibits angiogenic responses to hypoxia through a downregulation of vascular endothelial growth factor. Information on the sites where SRIF-sst_2 interactions take place is lacking, and downstream effectors mediating SRIF-sst_2 antiangiogenic actions are unknown.

METHODS. In the OIR model, retinal expression of SRIF was evaluated with RT-PCR and RIA. The bindings of [^{125}I]LTT-SRIF-28 and [^{125}I]Tyr^3-octreotide were measured in coronal sections of the eye. With Western blot we evaluated the levels of sst_{2A} as well as the expression and the activity of the Signal Transducer and Activator of Transcription (STAT)3. The analysis of STAT3 was performed in hypoxic mice treated with the sst_2 agonist octreotide or with the sst_2 antagonist D-Tyr^8 cyanamid 154806 (CYN). Retinal localization of sst_{2A} was assessed by single and double immunohistochemistry with an endothelial cell marker.

RESULTS. In the hypoxic retina, both SRIF and sst_2 levels as well as [^{125}I]Tyr^3-octreotide binding were downregulated. In addition, sst_{2A} immunostaining was decreased in the neuroretina, but was increased in capillaries. Hypoxia increased both expression and activity of STAT3. This increase was inhibited by octreotide, while was strengthened by CYN.

CONCLUSIONS. These data suggest that i. sst_2 expressed by capillaries may be responsible of the antiangiogenic effects of SRIF and ii. downstream effectors in this action include the transcription factor STAT3. These results support the possibility of using sst_2-selective ligands in the treatment of proliferative retinopathies and indicate STAT3 as an additional target for novel therapeutic approach.

Introduction

Angiogenic eye disease is among the most common causes of blindness worldwide and results from a profound imbalance between pro- and anti-angiogenic factors. Current treatments such as laser photocoagulation and administration of Vascular Endothelial Growth Factor (VEGF) inhibitors are insufficiently effective and there is now a great deal of interest to develop new and more efficacious therapeutic agents to treat ocular neovascularization. In this respect, analogues of the peptide somatostatin-14 (SRIF) may play a role in inhibiting angiogenesis in the retina.[1] In a mouse model of oxygen-induced retinopathy (OIR), we have recently demonstrated that the severity of angiogenic responses to hypoxia is correlated to the expression level of the SRIF receptor subtype 2 (sst_2) in the retina.[2] In fact, the lack of sst_2, as in sst_2-knock out (KO) retinas, is associated with heavier effects of hypoxia on retinal neovascularization and proangiogenic factors, whereas a chronic overexpression of sst_2 (consequent to the genetic deletion of sst_1 as in sst_1-KO retinas)[3,4] attenuates hypoxia effects on proangiogenic factors. In addition, we have observed, using the SRIF analogues octreotide (a sst_2-preferring agonist) and D-Tyr[8] cyanamid 154806 (CYN; a sst_2-specific antagonist), that sst_2 mediates SRIF antiangiogenic effects and that this mechanism involves a down regulation of retinal levels of VEGF.[5]

Although it is clear that SRIF analogues acting at sst_2 affect the expression of VEGF in the OIR model, information on the precise sites where this interaction may take place is surprisingly lacking. The most parsimonious way to explain the observed inhibitory effects of sst_2 agonists on VEGF expression and on the proliferation of retinal vessels would be to assume that sst_2 is expressed by retinal endothelial cells and that its interaction with VEGF takes place in these cells. However, localization studies of the mouse retina did not report sst_2 expression at the level of retinal blood capillaries,[6] nor has this expression been noted

in any other mammalian retinas,[7] although there is some evidence that sst_2 is localized to retinal vasculature in the human retina.[8,9] On the other hand, studies in human umbilical vein endothelial cells have shown that sst_2 and sst_5 are expressed in proliferating but not quiescent endothelial cells,[10] which suggests that these receptors may be upregulated in retinal capillaries in hypoxic conditions.

Despite the growing evidence that sst_2 agonists may exert angioinhibitory activity in the retina, the downstream effectors linking sst_2 activation to inhibition of angiogenic response or to modulation of VEGF expression are still unknown. Recent studies demonstrated that the Signal Transducer and Activator of Transcription (STAT)3 is critically involved in a wide variety of biological processes, including inflammation and angiogenesis. In the retina of OIR mice, for instance, protein levels of STAT3 and pSTAT3 are increased[11,12] with pSTAT3 preferentially localized to newly formed blood vessels.[12] In addition, retinal levels of both STAT3 and pSTAT3 are also increased in a mouse model of retinal ischemia.[13] Moreover, STAT3 phosphorylation is increased in retinal macrophages from OIR mice.[14] There are also results demonstrating that STAT3 is critical to modulate VEGF expression and activity in vascular endothelial cells, thus indicating a possible role of STAT3 in regulating angiogenic response to the hypoxic insult.[15-17]

In the present study, we determined whether low oxygen availability may affect levels and localization of sst_2 in the mouse retina and whether this effect may be related to altered levels of SRIF expression. In addition, we evaluated whether hypoxia affects expression and activity of STAT3 and whether the effects of hypoxia on STAT3 are influenced by treatment with the sst_2 agonist octreotide or the sst_2-selective antagonist CYN.

Materials and Methods

Octreotide was purchased from NeoMPS (Strasbourg, France). The iQ Sybr Green Supermix was from Bio-Rad (Hercules, CA). Primers were obtained from Eurofins MWG

Operon (Ebersberg, Germany). GelStar was from Cambrex (East Rutherford, NJ). LTT-SRIF-28 and Tyr^3-octreotide were obtained by Peninsula Laboratories (Meyerside, UK) and Gen Script Corporation (Piscataway, NJ), respectively. A rabbit polyclonal antibody directed to sst_{2A} was purchased from Gramsch Laboratories (Schwabhausen, Germany). In addition, a rat monoclonal antibody directed to CD31 was purchased from BD Pharmingen (San Diego, CA). A rabbit policlonal antibody to tyrosine hydroxylase (TH) was obtained from Chemicon (Temecula, CA). Appropriate secondary antibodies were from Molecular Probes (Eugene, OR). Rabbit polyclonal antibodies directed to STAT3 and pSTAT3 were obtained from Santa Cruz Biotechnologies (Santa Cruz, CA). The enhanced chemiluminescence reagent (WBKLS0500) was from Millipore (Billerica, MA). All other chemicals were obtained from Sigma-Aldrich (St. Louis, MO).

Animals

Experiments were performed on 68 mice (C57BL/6) of both sexes at postnatal day (PD) 17 (6 g body weight). In some experiments, mice at PD12 and PD14 were also used (15 animals for each age). Experiments were performed in agreement with the ARVO Statement for the Use of Animals in Ophthalmic and Vision Research and in compliance with the Italian law on animal care N°116/1992 and the EEC/609/86. All efforts were made to reduce the number of animals used.

Model of Oxygen-Induced Retinopathy

In a typical model of OIR,[18] litters of mice pups with their nursing mothers were exposed in an infant incubator to high oxygen concentration (75% ± 2%) between PD7 and PD12, prior to return to room air between PD12 and PD17. Oxygen was checked twice daily with an oxygen analyzer (Miniox I; Bertocchi srl Elettromedicali, Cremona, Italy). Individual litters were either oxygen or room air reared. In some experiments, pharmacological

treatment was also performed including no treatment, treatment with SRIF analogues and sham injection. Animals were treated with injections for 5 days from PD12 to PD16. Animals were anaestethized by i.p. injection of Avertin (1.2% tribromoethanol and 2.4% amylene hydrate in distilled water, 0.02 mL/g body weight). All experiments were performed at the same time of day to exclude possible circadian influences. The data were collected from both males and females and the results combined as there was no apparent gender difference.

Administration of SRIF Analogues

The sst_2-preferring peptidyl agonist octreotide and the sst_2-selective peptidyl antagonist CYN[19-21] were given twice daily subcutaneously from PD12 to PD16 at 0.02 mg kg^{-1} $dose^{-1}$ (octreotide) or at 0.5 mg kg^{-1} $dose^{-1}$ (CYN), as previously described.[5] The analogues were dissolved in 33 mM acetate buffer (pH 5) with 135 mM NaCl. Sham injections were performed with that vehicle.

Isolation of Retinal RNA and cDNA Preparation

Total RNA was extracted from explanted retinas (RNeasy Mini Kit; Qiagen, Valencia, CA), purified, resuspended in RNase-free water and quantified spectrophotometrically (SmartSpec 3000; Bio-Rad). First-strand cDNA was generated from 1 µg of total RNA (QuantiTect Reverse Transcription Kit; Qiagen).

Real-Time Quantitative RT-PCR

Real-time quantitative RT-PCR (QPCR) was performed according to Dal Monte et al.[5] SRIF primers (forward: CCCCAGACTCCGTCAGTTTCT, reverse: TCTCTGTCTGGTTGGGCTCG) were designed using Primer3 software,[22] whereas primer pairs for Rpl13a (forward: CACTCTGGAGGAGAAACGGAAGG, reverse:

GCAGGCATGAGGCAAACAGTC) were obtained from RTPrimerDB.[23] Amplification efficiency was close to 100% for both primer pairs as calculated (Opticon Monitor 3 software; Bio-Rad). SRIF target gene was run concurrently with Rpl13a, a constitutively expressed control gene. As previously described, samples were compared using the relative cycle threshold (CT method).[24] The increase or decrease (*x*-fold) was determinated relative to a control after normalizing to RPL13a. All reactions were run as triplicate. After statistical analysis, the data from the different experiments were plotted and averaged in the same graph. Data are expressed as means ± SE and originated from 4 samples for either control or hypoxic condition. Each sample refers to the mRNA extracted from 3 retinas.

SRIF Measurements

Explanted retinas were homogenized in 10 v/w acetic acid, 2 N. SRIF levels were evaluated by radioimmunoassay as previously described.[4,25] The results of the RIA assay are normalized for the amount of protein per retina and expressed as means ± SE from 6 retinas for either control or hypoxic conditions.

Autoradiography

For SRIF receptor autoradiography, LTT-SRIF-28 and Tyr^3-octreotide were iodinated as previously described[26] and used at a specific activity of 422 Ci/mmol and 662 Ci/mmol, respectively. Eyes from three control and three hypoxic mice were enucleated, quickly frozen in liquid nitrogen and stored at –80°C. Sections (16 µm) were cut on a cryostat. Receptor autoradiography was performed as previously described.[4] The sections were incubated in 545 pM [^{125}I]LTT-SRIF-28 or 260 pM [^{125}I]Tyr^3-octreotide. Non-specific binding was determined in a set of adjacent slides by incubation in the presence of 1 µM SRIF-14. Autoradiograms were generated by apposing the labelled sections to films

(BioMax MR; Kodak, Rochester, NY) at 4°C for 3 days. Photomicrographs of films were generated and analysed using a computerized image analysis system with the Mercator software (BIOCOM; Explora Nova-Mercator, La Rochelle, France). The autoradiographic quantification was expressed as pmol/retina surface and specific binding calculated as pmol/retina surface area unit assessed in total binding – pmol/retina surface area unit assessed in non-specific binding. Data are expressed as means ± SE and originated from 6 retinas for either control or hypoxic conditions.

Western Blotting

Western blot analysis was performed on proteins extracted from 3 samples for each experimental condition, according to Dal Monte et al.[5] Samples from age-matched control subjects were used for comparison. Each sample contained 5 retinas. Western blot analysis for STAT3 and pSTAT3 was performed on cytosolic proteins, extracted in buffer containing 0.1 mM sodium orthovanadate, 20 mM β-glycerophosphate and 20 mM p-nitrophenylphosphate. Western blot analysis for sst_{2A} was performed on the fraction containing membrane-bound proteins. Aliquots of each sample containing equal amounts of protein were subjected to SDS-PAGE on 10% acrylamide gels. β-actin was used as the loading control. Rabbit polyclonal antibodies directed to STAT3 (1:200 dilution) or sst_{2A} (1:500 dilution) or mouse monoclonal antibodies directed to pSTAT3 (1:200 dilution) or β-actin (1:2500 dilution) were used as primary antibodies. Mouse anti-rabbit horseradish peroxidase-labeled (1:5000 dilution) or rabbit anti-mouse horseradish peroxidase-labeled (1:25000 dilution) were used as secondary antibodies. Blots were developed with the enhanced chemiluminescence reagent, stripping them in between each assay. All experiments were run as duplicate. The semiquantitative analysis of Western blot signals was based on 3 independent blot-analysis experiments. After statistical analysis, data from the different experiments were plotted and averaged in the same graph.

Immunohistochemistry

The eyes were removed and immersion fixed in 4% paraformaldehyde in 0.1 M phosphate buffer (PB), pH 7.4, for 1 h. The fixed eyes were transferred to 25% sucrose in 0.1 M PB and stored at 4°C. Retinal sections were cut perpendicularly to the vitreal surface at 10 µm with a cryostat, mounted onto gelatin-coated slides and stored at -20°C. The rabbit antiserum against the sst_{2A} isoform was used at 1:500 dilution. In addition, a rat monoclonal antibody directed to the well known endothelial cell marker CD31 was used at 1:200 dilution for detection of retinal vessels.[27] Finally, a mouse monoclonal antibody to protein kinase C (PKC) was used at 1:200 to label rod bipolar cells, and a rabbit policlonal antibody to TH was used at 1:400 to label distinct wide-field amacrine cells.[6] The sections were incubated with the appropriate secondary antibody conjugated with Alexa Fluor 488 or Alexa Fluor 546 at a dilution of 1. Control experiments included the omission of the primary antibodies. Unspecific staining was not observed. In double labeling studies, control experiments were also performed to ensure that the primary antibodies did not cross-react when mixed together and that the secondary antibodies reacted only with the appropriate antigen-antibody complex. The immunofluorescence images were acquired using a 40x plan-NEOFLUAR Zeiss objective, an Axiocam photocamera and the Zeiss Axiovision 4 software (Carl Zeiss Vision GmbH, München-Hallbergmoos, Germany). The digital images were sized and optimized for contrast and brightness using Adobe Photoshop (Adobe Systems, Mountain View, CA, USA). Final images were saved at a minimum of 300 dpi. Quantitative analysis of double-labeled retinal sections was performed in agreement with Catalani et al.[28] Briefly, both the CD31- and the sst_{2A}-immunoreactive images relative to the same field were visualized. Subsequently, the images were turned into grayscale, normalized to the background and thresholded to obtain white immunostaining on black background. Using the KS-300 software (Carl

Zeiss), the area of CD31 immunostaining and that of sst_{2A}-immunoreactivity (IR) were calculated. Finally, the ratio between the area covered by the sst_{2A} staining and that covered by the CD31-IR was calculated and used as an index of the overlap area. Data are expressed as means ± SE and originated from 6 retinas for either control or hypoxic conditions.

Statistical Analysis

All data were analyzed by the Kolmogorov-Smirnov test on verification of normal distribution. Statistical significance was evaluated with unpaired t-test or with ANOVA followed by the Newman-Keuls multiple comparison test. The results are expressed as mean ± SE of the indicated *n* values (Prism; GraphPad Software, San Diego, CA). Differences with $P < 0.05$ were considered significant.

Results

Hypoxia Effects on SRIF

As shown in Figure 1A, RT-PCR yielded amplified products at 110 bp corresponding to SRIF mRNA. Five days of normoxia after hyperoxia (relative hypoxia) did not influence the amount of SRIF mRNA, which was similar to that in control retinas (Fig. 1B). In contrast, as shown in Figure 1C, SRIF levels measured by RIA were significantly decreased by hypoxia (~65% lower than in control retinas; $P < 0.05$).

Hypoxia Effects on sst_2 Binding and sst_{2A} Expression

The data summarized in Table 1 show high levels of SRIF binding sites in mouse retinas as the radioligand concentrations were in the picomolar range. Non-specific binding was low for both radioligands used. In hypoxic retinas, [^{125}I]LTT-SRIF-28 binding sites were not

significantly different from the respective values in control retinas. In contrast, [^{125}I]Tyr^{3}-octreotide binding sites were significantly decreased by ~30% (Fig. 2, Table 1).

Regarding the levels of sst_{2A}, semiquantitative Western blot showed that they were not significantly different from control values both at PD12 (end of the period of hyperoxia) and at PD14 (2 days of normoxia). In contrast, 5 days after hyperoxia (relative hypoxia, PD17), retinal levels of sst_{2A} were significantly lower than those in control conditions (~26%, $P < 0.05$; Fig. 3).

Hypoxia Effects on sst_{2A} Localization

The immunostaining patterns of sst_{2A} in control retinas were consistent with previous observations of the mouse retina.[3,4,29] In particular, sst_{2A}-IR was mostly localized to rod bipolar cells and to amacrine cells, whereas it was scarcely associated to retinal capillaries labeled with CD31 (Figs. 4A,C). Hypoxia caused a drastic reduction of sst_{2A} immunostaining in retinal neurons accompanied by an evident increase of sst_{2A}-IR in retinal blood vessels (Figs. 4B,D). Retinal vasculature includes three layers of capillary networks: the most superfical layer of capillaries lying in the inner part of the nerve fiber layer (NFL), the inner capillaries which lie in the ganglion cell layer (GCL), and the outer capillary network which runs from the inner plexiform layer (IPL) to the outer plexiform layer (OPL) through the inner nuclear layer (INL).[30] As shown in Figure 4E, the mean overlap area covered by sst_{2A}-IR and CD31-IR almost doubled in the IPL-INL of hypoxic retinas in respect with control retinas. In contrast, hypoxia did not affect the mean overlap area in the NFL-GCL. Additional experiments were performed to determine whether hypoxia-induced decrease of sst_{2A}-IR might result from hypoxia-induced alterations of the retinal cells which are known to express sst_{2A}. In the rodent retina, sst_{2A} is in TH-containing amacrine cells and in rod bipolar cells, as identified by PKC-IR.[31] As shown in figure 5, hypoxia did not influence the TH nor the PKC immunostaining patterns.

Hypoxia Effects on STAT3

As shown in Figure 6, STAT3 was more than doubled in the hypoxic samples as compared to controls ($P < 0.001$). Similarly, pSTAT3 was also significantly increased in the hypoxic retina as compared to control retina (~133%, $P < 0.001$). Vehicle treatment did not affect retinal levels of STAT3 or of pSTAT3, while octreotide significantly decreased both STAT3 and pSTAT3 (~28% and 26%, respectively, $P < 0.001$) in the hypoxic retina. In contrast, CYN significantly increased pSTAT3 levels (~10%, $P < 0.05$) without affecting STAT3.

Discussion

The results of this study demonstrate for the first time that in the OIR model hypoxia upregulates sst_{2A} expression by retinal vessels suggesting that the growing endothelium overexpresses sst_{2A} and becomes capable to efficiently respond to the angioinhibitory action of SRIF. The present findings also indicate that hypoxia upregulates STAT3 expression and activity in the OIR model and suggest that STAT3 plays an important role in mediating sst_2 action in proliferative retinopathy.

Hypoxia Effects on SRIF

As shown herein, retinal levels of SRIF are downregulated in the OIR model. This result is consistent with decreased SRIF levels observed in the vitreous and/or in the retina of diabetic patients,[32-34] and concurs to demonstrate that ocular deficit of SRIF may contribute to the onset of diabetic retinopathy. In this respect, protective effects of SRIF and its analogues have been recently demonstrated in rodent models of retinal neurodegeneration.[28,35,36]

The fact that, following hypoxia, endogenous SRIF decreases in the retina, whereas SRIF mRNA does not change suggests a downregulation at the post-transcriptional level, involving transduction pathways that do not interact with nuclear regulatory factors. This possibility is consistent with previous findings suggesting the involvement of post-translational mechanisms in the regulation of SRIF expression in the retina of mice with genetic deletion of the SRIF receptors sst_1 or sst_2.[3,4]

Hypoxia Effects on sst_2

Our results show that hypoxia downregulates retinal levels of the sst_{2A} isoform of sst_2, suggesting that sst_{2A} downregulation is associated with the onset of angiogenesis in the retina of the OIR mouse model. That hypoxia might regulate the expression of cell surface receptors has been demonstrated, in different experimental models, for the adenosine receptors of the A_{2A} subtype,[37] the delta opioid receptors,[38] and the glucocorticoid receptors.[39] However, to the best of our knowledge no results are available reporting hypoxia-induced regulation of SRIF receptors. As shown herein, sst_{2A} reduction is not accompanied by changes in sst_2 gene expression, as demonstrated by previous findings,[2] indicating the involvement of translational or post-translational mechanisms.

Our autoradiographic studies confirmed the decrease of sst_2 protein levels in hypoxic retinas and showed a marked decrease in [^{125}I]Tyr^3-octreotide binding sites. Although [^{125}I]Tyr^3-octreotide labels with high affinity both recombinant sst_2 and sst_5,[40] the observed binding is likely to be due entirely to the presence of sst_2.[4] Since [^{125}I]LTT-SRIF-28 labels with high affinity all SRIF receptors,[40] the fact that in control retinas [^{125}I]LTT-SRIF-28 binding sites have a density similar to that in hypoxic retinas suggests that the total number of SRIF receptors does not change as a consequence of hypoxia, and implies that the decrease of sst_2 following hypoxia is compensated by an increase in the levels of other

SRIF receptors. Indeed, a major effect of sst_2 loss on the expression of sst_1 has been demonstrated previously in the mouse retina.[3]

The mechanisms leading to reduced sst_2 levels in hypoxic retinas remain to be elucidated. It is likely that SRIF, sst_1 and sst_2 cooperate in complex regulatory mechanisms controlling their own expressions in the retina (for discussion, see Ref. 3). Our previous observations indicate a strict correlation between retinal SRIF levels and sst_2 expression,[3,4] but at present it is difficult to determine whether an effect of hypoxia on SRIF retinal levels would, in turn, affect sst_2 expression or, conversely, an effect of hypoxia on sst_2 would affect SRIF levels in the retina. On the other hand, in the mouse retina, the possibility that SRIF levels are regulated by sst_2 seems unlikely since only sst_1 is expressed by SRIF-containing amacrine cells.[4,41,42]

Dynamic Changes of sst_{2A} Localization After Hypoxia

The localization studies demonstrate for the first time that hypoxia induces a drastic reduction in sst_{2A}-IR in retinal cells and processes. Although acute exposure to hypoxia was recently shown to cause changes in Muller cells and degeneration of neural cells in the retina of neonatal rats,[43] the persistence of the cells known to express sst_{2A}, including amacrine and rod bipolar cells,[6] excludes the possibility that in the OIR model the observed reduction of sst_{2A} is caused by hypoxic damage to the cells expressing the receptor.

We observed that in hypoxic retinas endothelial cells display relatively abundant sst_{2A}-IR, whereas in normoxic retinas sst_{2A}-IR is scarcely associated with retinal vessels. This result is in line with the finding that quiescent human vascular endothelial cells do not express sst_2 and this receptor is expressed when the endothelial cells begin to grow.[10,44] In addition, our observations are also consistent with studies in human eyes with choroidal neovascularization, where newly formed endothelial cells strongly express sst_2.[9] Finally,

the pattern of sst_2 expression in patients with diabetic retinopathy indicates that beneficial effects of sst_2 agonists may depend on the presence of sst_2 on newly-formed vessels.[45] Our results on hypoxia-induced upregulation of sst_{2A} expression in retinal vessels suggest that sst_{2A} in the growing endothelium can receive angioinhibitory action of SRIF analogues with high affinity for sst_2. A relationship between sst_2 levels and octreotide efficacy has recently been demonstrated in rats with advanced stages of portal hypertension in which sst_2 becomes downregulated and this downregulation can be responsible of the failure of octreotide therapy to inhibit angiogenesis.[46]

STAT3 as Downstream Effector

Our recent work demonstrates that SRIF angioinhibitory effects initiated by sst_2 activation involve down regulation of VEGF expression.[5] Consistent with such observations, octreotide has been found to be effective in reducing both choroidal neovascularization and VEGF mRNA levels in retinal pigment epithelium and choroidal tissue of rats.[47] Therefore, it would be important to detect downstream effectors to trace a link between sst_2 activation and VEGF modulation. Much work has been done to clarify the functional role of transcription factors regulating target genes involved in angiogenesis.[27,48,49] Of these transcription factors, STAT3 appears of particular interest because its activation appears to be coupled to regulation of VEGF.[16,50-53]

STAT3 has been detected in the retina, although its role there has not been entirely determined.[13,54,55] STAT3 expression and activation are increased in the OIR model,[11,12,14] and activated STAT3 has been localized to retinal neovascular vessels.[12] In line with these results, we demonstrated that both STAT3 and pSTAT3 are upregulated by hypoxia in OIR mice suggesting that STAT3 may help to mediate proliferation of blood vessels in the neovascular retina.

As also shown here, upregulation of STAT3 in the hypoxic retina is influenced by treatment with sst_2 agonist or antagonist. In fact, the hypoxia-induced increase of both STAT3 and pSTAT3 is consistently reduced by sst_2 activation with octreotide, indicating that ameliorative effects of octreotide on angiogenic responses in the hypoxic retina are likely to involve STAT3 production. In the OIR model, beneficial effects of statins on retinal neovascularization have been reported to be associated with statin effects in preventing pSTAT3 upregulation.[11] In addition, in rats treated with streptozotocin to induce diabetes and in retinal endothelial cells maintained in high-glucose medium the ameliorative effects of simvastatin seem to prevent STAT3 activation.[56]

Our demonstration that octreotide prevents the upregulation of pSTAT3 associated with neovascularization in the OIR model is in line with previous results showing an inhibitory effect of octreotide on STAT3 activity in myeloid cells.[57] This inhibitory effect includes the activation of Src homology region 2 domain-containing phosphatase 1 (SHP-1), which in turn inhibits STAT3 activation. Interestingly, SHP-1 has been reported to be associated with the antiproliferative effect of sst_2 in tumor cells (for a review, see Ref. 58). Our additional finding that the hypoxia-induced increase in pSTAT3 is further enhanced by sst_2 blockade with CYN adds further evidence supporting sst_2 coupling to STAT3 in the mouse retina. Although there is indication of possible STAT3 location downstream of VEGF,[11,12] we favour the hypothesis that the sst_2-induced inhibition of angiogenesis occurs through sst_2 functional coupling to STAT3 which, in turn, causes VEGF downregulation. The possibility that STAT3 activation is an upstream event with respect to hypoxia-induced VEGF upregulation is also suggested by results in bovine microvascular endothelial cells in which the activation of STAT3 is required to mediate the effects of peroxynitrite in stimulating VEGF expression.[15] Additional investigations are necessary to verify the role of STAT3 in mediating inhibitory effects of sst_2 activation on retinal angiogenesis and VEGF

expression. Delineating the pathway by which STAT3 mediates sst_2 action in retinal angiogenesis may provide new targets for pharmacologic modulation of angiogenesis.

Conclusion

SRIF analogues with high specificity for sst_2 exert antiangiogenic effects by interfering with the VEGF system in the OIR model. Here, we demonstrate that low oxygen availability affects levels and localization of sst_2 in the mouse retina and that this effect may be related to altered levels of SRIF. We also demonstrate that hypoxia influences expression and activity of STAT3 and that hypoxia effects on STAT3 are reduced by sst_2 activation with octreotide. We suggest the possibility that sst_2 expressed by retinal capillaries exerts its angioinhibitory action through STAT3-induced modulation of VEGF. The present results further support the possibility of the use of sst_2-selective ligands in the treatment of retinopathy. Considering the eminent function of STAT3 in retinopathy, its targeting may represent a novel strategy for therapeutic intervention. However, it is important to underline that although the OIR model used in the present study manifests the symptoms of retinal angiogenesis, it is not a model of proliferative diabetic retinopathy (PDR) as the angiogenesis associated with PDR may well involve different mechanism(s) in diabetes

Acknowledgements

We wish to thank Dr. Maurizio Cammalleri for his help in the pharmacological treatment of the animals. We also thank Dr. Angelo Gazzano and Gino Bertolini for assistance with mouse colonies.

References

1. Hernandez C, Simò R. Strategies for blocking angiogenesis in diabetic retinopathy: from basic science to clinical practice. *Expert Opin Investig Drugs*. 2007;16:1209-1226.
2. Dal Monte M, Cammalleri M, Martini D, Casini G, Bagnoli P. Antiangiogenic role of somatostatin receptor 2 in a model of hypoxia-induced neovascularization in the retina: results from transgenic mice. *Invest Ophthalmol Vis Sci*. 2007;48:3480-3489.
3. Casini G, Dal Monte M, Petrucci C, et al. Altered morphology of rod bipolar cell axonal terminals in the retinas of mice carrying genetic deletion of somatostatin subtype receptor 1 or 2. *Eur J Neurosci*. 2004;19:43-54.
4. Dal Monte M, Petrucci C, Vasilaki A, et al. Genetic deletion of somatostatin receptor 1 alters somatostatinergic transmission in the mouse retina. *Neuropharmacology*. 2003;45:1080-1092.
5. Dal Monte M, Ristori C, Cammalleri M, Bagnoli P. Somatostatin analogs affect retinal angiogenesis in a mouse model of oxygen-induced retinopathy: involvement of the somatostatin receptor subtype 2. *Invest Ophthalmol Vis Sci*. 2009;50:3596-3606.
6. Cristiani R, Petrucci C, Dal Monte M, Bagnoli P. Somatostatin (SRIF) and SRIF receptors in the mouse retina. *Brain Res*. 2002;936:1-14.
7. Bagnoli P, Dal Monte M, Casini G. Expression of neuropeptides and their receptors in the developing retina of mammals. *Histol Histopathol*. 2003;18:1219-1242.
8. Klisovic DD, O'Dorisio MS, Katz SE, et al. Somatostatin receptor gene expression in human ocular tissues: RT-PCR and immunohistochemical study. *Invest Ophthalmol Vis Sci*. 2001;42:2193-2201.
9. Lambooij AC, Kuijpers RW, van Lichtenauer-Kaligis EG, et al. Somatostatin receptor 2A expression in choroidal neovascularization secondary to age-related macular degeneration. *Invest Ophthalmol Vis Sci*. 2000;41:2329-2335.

10. Adams RL, Adams IP, Lindow SW, Zhong W, Atkin SL. Somatostatin receptors 2 and 5 are preferentially expressed in proliferating endothelium. *Br J Cancer*. 2005;92:1493-1498.
11. Bartoli M, Al-Shabrawey M, Labazi M, et al. HMG-CoA reductase inhibitors (statin) prevents retinal neovascularization in a model of oxygen-induced retinopathy. Invest Ophthalmol Vis Sci. 2009;50:4934-4940.
12. Mechoulam H, Pierce EA. Expression and activation of STAT3 in ischemia-induced retinopathy. *Invest Ophthalmol Vis Sci*. 2005;46:4409-4416.
13. Zhang C, Li H, Liu MG et al. STAT3 activation protects retinal ganglion cell layer neurons in response to stress. *Exp Eye Res.* 2008;86:991-997.
14. Dace DS, Khan AA, Kelly J, Apte RS. Interleukin-10 promotes pathological angiogenesis by regulating macrophage response to hypoxia during development. PLoS One. 2008;3:e3381.
15. Platt DH, Bartoli M, El-Remessy AB et al. Peroxynitrite increases VEGF expression in vascular endothelial cells via STAT3. *Free Radic Biol Med.* 2005;39:1353-1361.
16. Bartoli M, Platt D, Lemtalsi T, et al. VEGF differentially activates STAT3 in microvascular endothelial cells. *FASEB J*. 2003;17:1562-1564.
17. Bartoli M, Gu X, Tsai NT, et al. Vascular endothelial growth factor activates STAT proteins in aortic endothelial cells. J Biol Chem. 2000;275:33189-33192.
18. Smith LEH, Wesolowski E, McLellan A, et al. Oxygen-induced retinopathy in the mouse. *Invest Ophtalmol Vis Sci*. 1994;35:101-111.
19. Olias G, Viollet C, Kusserow H, Epelbaum J, Meyerhof W. Regulation and function of somatostatin receptors. *J Neurochem*. 2004;89:1057-1091.
20. Nunn C, Schoeffer P, Langenegger D, Hoyer D. Functional characterisation of the putative somatostatin sst2 receptor antagonist CYN 154806. *Naunyn Schmiedebergs Arch Pharmacol*. 2003;367:1-9.

21. Weckbecker G, Lewis I, Albert R, Schmid HA, Hoyer D, Bruns C. Opportunities in somatostatin research: biological, chemical and therapeutic aspects. *Nat Rev Drug Discov*. 2003;2:999-1017.

22. Rozen S, Skaletsky H. Primer3 on the WWW for general users and for biologist programmers. *Methods Mol Biol*. 2000;132:365-386.

23. Pattyn F, Speleman F, De Paepe A, Vandesompele J. RTPrimerDB: the real-time PCR primer and probe database. *Nucleic Acids Res*. 2003;31:122-123.

24. Livak KJ, Schmittgen TD. Analysis of relative gene expression data using real-time quantitative PCR and the 2(-Delta Delta C(T)) Method. *Methods*. 2001;25:402-408.

25. Grouselle D, Winsky-Sommerer R, David JP, Delacourte A, Dournaud P, Epelbaum J. Loss of somatostatin-like immunoreactivity in the frontal cortex of Alzheimer patients carrying the apolipoprotein epsilon 4 allele. *Neurosci Lett*. 1998;255:21-24.

26. Moyse E, Beaudet A, Bertherat J, Epelbaum J. Light microscopic radioautographic localization of somatostatin binding sites in the brainstem of the rat. *J Chem Neuroanat*. 1992;5:75-84.

27. DeNiro M, Alsmadi O, Al-Mohanna F. Modulating the hypoxia-inducible factor signaling pathway as a therapeutic modality to regulate retinal angiogenesis. *Exp Eye Res*. 2009;89:700-717.

28. Catalani E, Cervia D, Martini D, et al. Changes in neuronal response to ischemia in retinas with genetic alterations of somatostatin receptor expression. *Eur J Neurosci*. 2007;25:1447-1459.

29. Mastrodimou N, Vasilaki A, Papadioti A, Low MJ, Hoyer D, Thermos K. Somatostatin receptors in wildtype and somatostatin deficient mice and their involvement in nitric oxide physiology in the retina. *Neuropeptides*. 2006;40:365-373.

30. Zhang HR. Scanning electron-microscopic study of corrosion casts on retinal and choroidal angioarchitecture in man and animals. *Prog Ret Eye Res*. 1994;13:243-270.

31. Cervia D, Casini G, Bagnoli P. Physiology and pathology of somatostatin in the mammalian retina: a current view. Mol Cell Endocrinol. 2008;286:112-122.
32. Carrasco E, Hernández C, Miralles A, Huguet P, Farrés J, Simó R. Lower somatostatin expression is an early event in diabetic retinopathy and is associated with retinal neurodegeneration. *Diabetes Care*. 2007;30:2902-2908.
33. Hernandez C, Carrasco E, Casamitjana R, Deulofeu R, García-Arumí J, Simó R. Somatostatin molecular variants in the vitreous fluid: a comparative study between diabetic patients with proliferative diabetic retinopathy and nondiabetic control subjects. *Diabetes Care*. 2005;28:1941-1947.
34. Simó R, Lecube A, Sararols L, et al. Deficit of somatostatin-like immunoreactivity in the vitreous fluid of diabetic patients: possible role in the development of proliferative diabetic retinopathy. *Diabetes Care*. 2002;25:2282-2286.
35. Cervia D, Martini D, Ristori C, et al. Modulation of the neuronal response to ischaemia by somatostatin analogues in wild-type and knock-out mouse retinas. *J Neurochem*. 2008;106:2224-2235.
36. Kiagiadaki F, Thermos K. Effect of intravitreal administration of somatostatin and sst2 analogs on AMPA-induced neurotoxicity in rat retina. *Invest Ophthalmol Vis Sci*. 2008;49:3080-3089.
37. Feoktistov I, Ryzhov S, Zhong H, et al. Hypoxia modulates adenosine receptors in human endothelial and smooth muscle cells toward an A2B angiogenic phenotype. *Hypertension*. 2004;44:649-654.
38. Zhu M, Li MW, Tian XS, Ou XM, Zhu CQ, Guo JC. Neuroprotective role of delta-opioid receptors against mitochondrial respiratory chain injury. *Brain Res*. 2009;1252:183-191.

39. Huang Y, Zhao JJ, Lv YY, Ding PS, Liu RY. Hypoxia down-regulates glucocorticoid receptor alpha and attenuates the anti-inflammatory actions of dexamethasone in human alveolar epithelial A549 cells. Life Sci. 2009;85:107-112.
40. Siehler S, Seuwen K, Hoyer D. Characterisation of human recombinant somatostatin receptors. 1. Radioligand binding studies. *Naunyn Schmiedebergs Arch Pharmacol*. 1999;360:488-499.
41. Thermos K, Bagnoli P, Epelbaum J, Hoyer D. The somatostatin sst1 receptor: an autoreceptor for somatostatin in brain and retina? *Pharmacol Ther*. 2006;110:455-464.
42. Cristiani R, Fontanesi G, Casini G, Petrucci C, Viollet C, Bagnoli P. Expression of somatostatin subtype 1 receptor in the rabbit retina. *Invest Ophthalmol Vis Sci*. 2000;41:3191-3199.
43. Kaur C, Sivakumar V, Foulds WS, Luu CD, Ling EA. Cellular and vascular changes in the retina of neonatal rats following an acute exposure to hypoxia. *Invest Ophthalmol Vis Sci*. 2009;50:5364-5374.
44. Watson JC, Balster DA, Gebhardt BM, et al. Growing vascular endothelial cells express somatostatin subtype 2 receptors. *Br J Cancer*. 2001;85:266-272.
45. van Hagen PM, Baarsma GS, Mooy CM, et al. Somatostatin and somatostatin receptors in retinal diseases. *Eur J Endocrinol*. 2000;143 Suppl 1:S43-51.
46. Mejias M, Garcia-Pras E, Tiani C, Bosch J, Fernandez M. The somatostatin analogue octreotide inhibits angiogenesis in the earliest, but not in advanced, stages of portal hypertension in rats. *J Cell Mol Med*. 2008;12:1690-1699.
47. Qu Y, Zhang S, Xu X, et al. Octreotide inhibits choroidal neovascularization in rats.*Ophthalmic Res*. 2009;42:36-42.
48. Guma M, Rius J, Duong-Polk KX, Haddad GG, Lindsey JD, Karin M. Genetic and pharmacological inhibition of JNK ameliorates hypoxia-induced retinopathy through interference with VEGF expression. *Proc Natl Acad Sci USA*. 2009;106:8760-8765.

49. Phng LK, Potente M, Leslie JD, et al. Nrarp coordinates endothelial Notch and Wnt signaling to control vessel density in angiogenesis. *Dev Cell*. 2009;16:70-82.

50. Noman MZ, Buart S, Van Pelt J, et al. The cooperative induction of hypoxia-inducible factor-1 alpha and STAT3 during hypoxia induced an impairment of tumor susceptibility to CTL-mediated cell lysis. *J Immunol*. 2009;182:3510-3521.

51. Gray MJ, Zhang J, Ellis LM, et al. HIF-1alpha, STAT3, CBP/p300 and Ref-1/APE are components of a transcriptional complex that regulates Src-dependent hypoxia-induced expression of VEGF in pancreatic and prostate carcinomas. *Oncogene*. 2005;24:3110-3120.

52. Niu G, Wright KL, Huang M, Song L, Haura E, et al. Constitutive Stat3 activity up-regulates VEGF expression and tumor angiogenesis. *Oncogene*. 2002;21:2000-2008.

53. Schaefer LK, Ren Z, Fuller GN, Schaefer TS. Constitutive activation of Stat3alpha in brain tumors: localization to tumor endothelial cells and activation by the endothelial tyrosine kinase receptor (VEGFR-2). *Oncogene*. 2002;21:2058-2065.

54. Ozawa Y, Nakao K, Kurihara T et al. Roles of STAT3/SOCS3 pathway in regulating the visual function and ubiquitin-proteasome-dependent degradation of rhodopsin during retinal inflammation. *J Biol Chem* 2008;283:24561-24570.

55. Ueki Y, Wang J, Chollangi S, Ash JD. STAT3 activation in photoreceptors by leukemia inhibitory factor is associated with protection from light damage. *J Neurochem* 2008;105:784-796.

56. Al-Shabrawey M, Bartoli M, El-Remessy AB, et al. Role of NADPH oxidase and Stat3 in statin-mediated protection against diabetic retinopathy. Invest Ophthalmol Vis Sci. 2008;49:3231-3238.

57. Oomen SP, Ward AC, Hofland LJ, Lamberts SW, Löwenberg B, Touw IP. Somatostatin modulates G-CSF-induced but not interleukin-3-induced proliferative

responses in myeloid 32D cells via activation of somatostatin receptor subtype 2. *Hematol J*. 2001;2:322-329.

58. Florio T. Somatostatin/somatostatin receptor signalling: phosphotyrosine phosphatases. *Mol Cell Endocrinol*. 2008;286:40-48.

TABLE 1. Autoradiographic analysis of SRIF binding sites from both control and hypoxic mouse retinas

Radioligand	Specific binding	
	control	hypoxic
[^{125}I]LTT-SRIF-28	3.91 ± 0.16	3.67 ± 0.28
[^{125}I]Tyr^{3}-octreotide	3.51 ± 0.26	2.83 ± 0.08*

The data are expressed as specific binding (pmol/retina surface area unit assessed in total binding – pmol/retina surface area unit assessed in non-specific binding) ± SE of 12-17 coronal sections. *P < 0.05 versus the respective control (unpaired t-test)

Legends

FIGURE 1. Retinal levels of SRIF in hypoxic mice. (**A**) PCR products of SRIF mRNA (110 bp) and the housekeeping gene Rpl13a (182 bp) in normoxic control retinas. (**B**) SRIF mRNA in control (*white*) and hypoxic (*black*) conditions. QPCR evaluation showed that SRIF messenger was not influenced by hypoxia. Data were analyzed by the formula $2^{-\Delta\Delta CT}$ using Rpl13a as internal standard. Each column represents the mean ± SE of data from 4 samples. Each sample refers to the mRNA extracted from 3 retinas. (**C**) Endogenous level of SRIF in the retina of control (*white*) and hypoxic (*black*) mice. RIA measurement showed that SRIF level was decreased by hypoxia (*P < 0.05 versus control; unpaired *t*-test). The amount of SRIF is expressed as pg/mg of proteins. Each column represents the mean ± SE of data from 6 retinas.

FIGURE 2. Representative photomicrographs of the autoradiographic signals of [^{125}I]LTT-SRIF-28- (**A-B**) and [^{125}I]Tyr^3-octreotide- (**C-D**) labelled binding sites in coronal sections of control (**A, C**) and hypoxic (**B, D**) mouse eyes. Total and non-specific are sequential sections from the same eye and determined as described in the experimental procedures. Note that hypoxia causes a decrease in [^{125}I]Tyr^3-octreotide-labelled binding sites. I: iris, P: posterior eye (sclera, choroid), R: retina. Scale bar: 1 mm.

FIGURE 3. Levels of sst_{2A} in normoxic (*white*) and hypoxic (*black*) conditions, as evaluated by Western blot using β-actin as the loading control in mouse retinas. Densitometric analysis showed that sst_{2A} was decreased by hypoxia at postnatal day (PD) 17 which corresponds to 5 days of normoxia after hyperoxia (*P < 0.05 versus the respective control; ANOVA followed by Newman-Keuls multiple comparison post test). No effects were observed at PD 12 which corresponds to the end of hyperoxia (*dashed*) or at PD 14

which corresponds to 2 days of normoxia after hyperoxia. Each column represents the mean ± SE of data from 3 samples. Each sample refers to the protein extracted from 5 retinas. Representative gels are also shown and are numbered progressively in correspondence with the histograms.

FIGURE 4. Retinal sections showing cell and capillary profiles immunoreactive for sst_{2A} (**A, B**) and CD31 (**C, D**) in control (**A, C**) and hypoxic (**B, D**) conditions. Arrows point to retinal vessel profiles double-labeled with sst_{2A} and CD31. Scale bar: 20 µm. (**E**) Mean overlap area covered by sst_{2A}- and CD31-IR in control (*white*) and hypoxic (*black*) conditions. Histograms shows that the overlap area is increased by hypoxia in IPL-INL but not in NFL-GCL (*P < 0.001 vs control; unpaired t-test). Each histogram represents the mean ± SE of data from 6 retinas from either control or hypoxic mice. Abbreviations: ONL, outer nuclear layer; OPL, outer plexiform layer; INL, inner nucler layer; IPL, inner plexiform layer; GCL, ganglion cell layer; NFL, nerve fiber layer.

FIGURE 5. Retinal sections showing TH (**A, B**) and PKC (**C, D**) immunolabelling in control (**A, C**) and hypoxic (**B, D**) conditions. Scale bar, 20 µm. For abbreviations, see the legend of Figure 4.

FIGURE 6. Levels of STAT3 (**A**) and pSTAT3 (**B**) in hypoxic retinas after treatment with vehicle, 0.02 mg Kg^{-1} octreotide or 0.5 mg Kg^{-1} CYN, as evaluated by Western blot using β-actin as the loading control. (**A, B**) Densitometric analysis showed that both STAT3 and pSTAT3 were increased by hypoxia (*P < 0.001 versus the respective control; ANOVA followed by Newman-Keuls multiple comparison post test). STAT3 level in vehicle-treated mice was not significantly different from that in hypoxic mice. The hypoxia-induced increase in both STAT3 and pSTAT3 was significantly lowered by octreotide (§§P < 0.001

versus the respective vehicle-treated; ANOVA followed by Newman-Keuls multiple comparison post test). The hypoxia induced increase of STAT-3 was unaffected by CYN whereas the hypoxia induced increase in pSTAT3 was increased by CYN ($^{\S}P < 0.05$ versus the respective vehicle-treated; ANOVA followed by Newman-Keuls multiple comparison post test). Each column represents the mean ± SE of data from 3 samples. Each sample refers to the protein extracted from 5 retinas. Representative gels are also shown.

Figure 1.

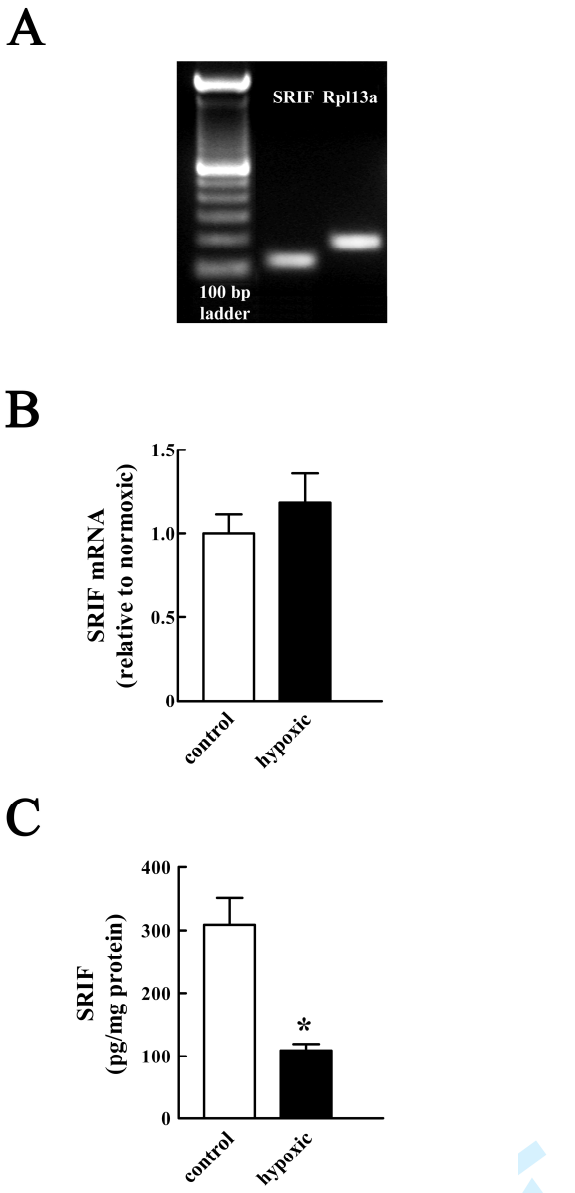
A
SRIF Rpl13a
100 bp ladder
B
SRIF mRNA (relative to normoxic)
1.5
1.0
0.5
0
control
hypoxic
C
SRIF (pg/mg protein)
400
300
200
100
0
*
control
hypoxic

Figure 2.

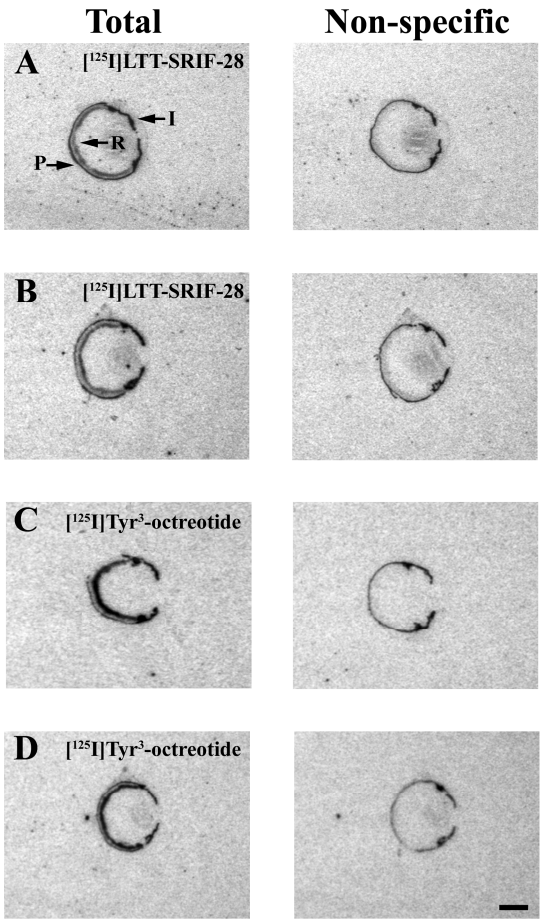
Total
Non-specific
A
[125I]LTT-SRIF-28
I
R
P
B
[125I]LTT-SRIF-28
C
[125I]Tyr3-octreotide
D
[125I]Tyr3-octreotide

Figure 3.

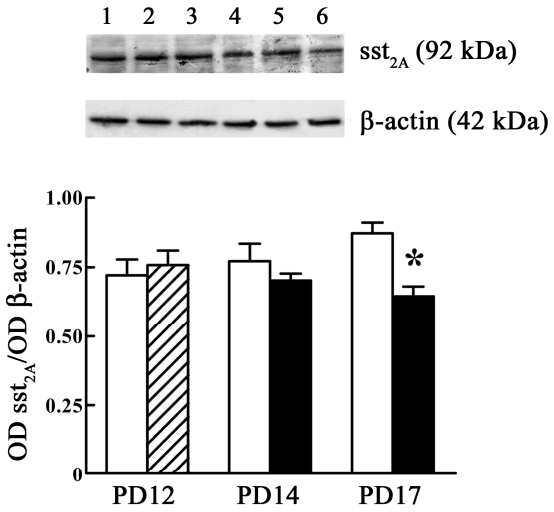

Figure 4.

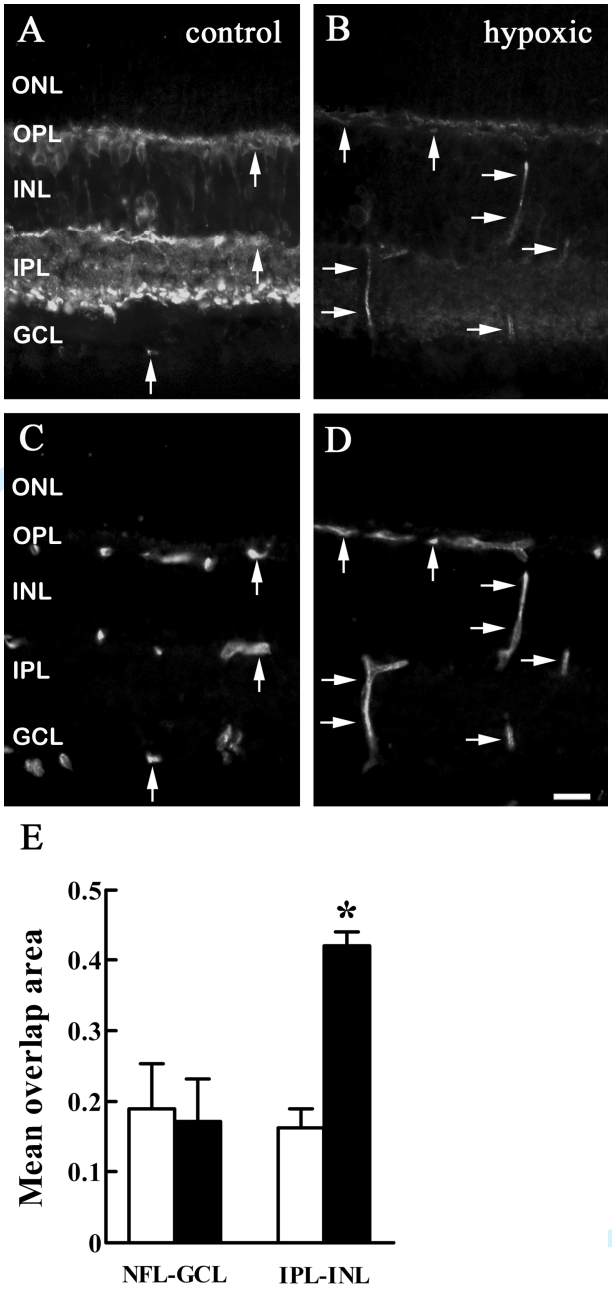
A
control
ONL
OPL
INL
IPL
GCL
B
hypoxic
C
ONL
OPL
INL
IPL
GCL
D
E
Mean overlap area
0.5
0.4
0.3
0.2
0.1
0
*
NFL-GCL
IPL-INL

Figure 5.

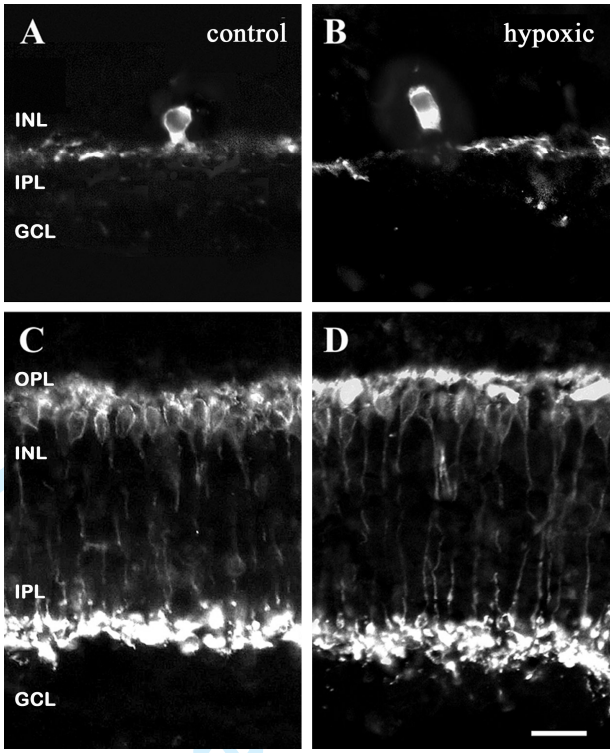

Figure 6.

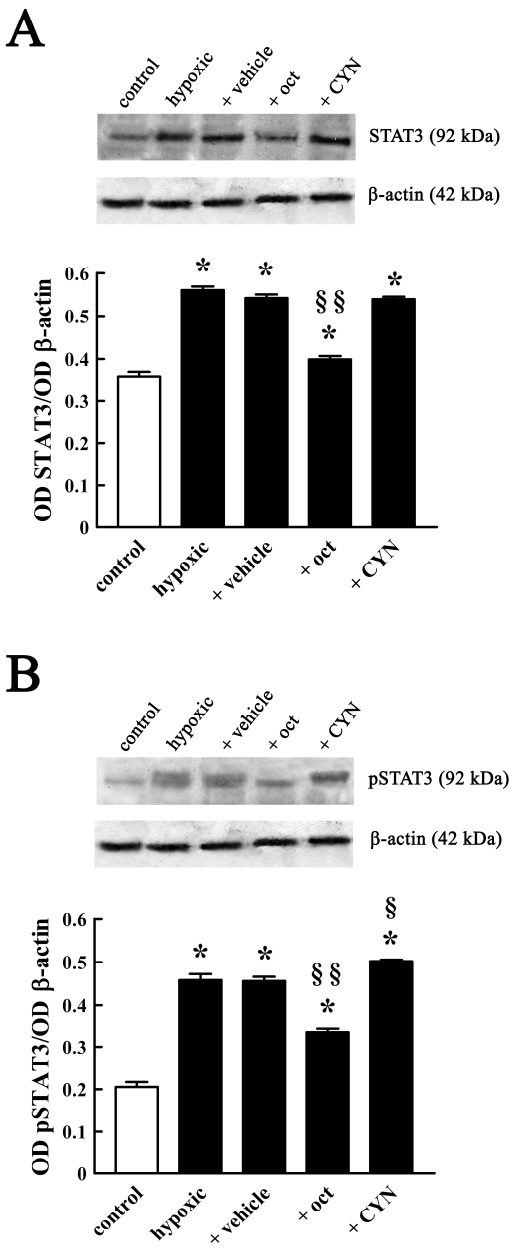
A
control
hypoxic
+ vehicle
+ oct
+ CYN
STAT3 (92 kDa)
β-actin (42 kDa)
OD STAT3/OD β-actin
0.6
0.5
0.4
0.3
0.2
0.1
0
*
*
§§
*
*
control
hypoxic
+ vehicle
+ oct
+ CYN
B
control
hypoxic
+ vehicle
+ oct
+ CYN
pSTAT3 (92 kDa)
β-actin (42 kDa)
OD pSTAT3/OD β-actin
0.6
0.5
0.4
0.3
0.2
0.1
0
*
*
§§
*
§
*
control
hypoxic
+ vehicle
+ oct
+ CYN